ORCA – Online Research @ Cardiff

Resource potential of gas reservoirs in South Pakistan and adjacent Indian subcontinent revealed by post-stack inversion techniques

Aamir Ali[1], Tiago M. Alves[2*], Farhad Aslam Saad[1], Matee Ullah[1], Muhammad Toqeer[1], Matloob Hussain[1]

[1]Department of Earth Sciences, Quaid-i-Azam University, 45320, Islamabad, Pakistan

[2]3D Seismic Lab, School of Earth and Ocean Sciences, Cardiff, University, CF10 3AT, United Kingdom.

*AlvesT@cardiff.ac.uk

ABSTRACT

Seismic post-stack inversion facilitates the interpretation, mapping and quantification of hydrocarbon bearing zones. This study estimates reservoir properties (i.e. acoustic impedance and porosity) by applying post-stack seismic inversion techniques to a gas prone reservoir in the Sawan area, Southern Indus Basin, Pakistan. In this particular study, model-based and sparse-spike inversion algorithms are successfully applied on 3D seismic and wireline log data to predict reservoir character in the Lower Goru Formation (C-sand interval). Our results suggest that model-based post-stack seismic inversions provide reasonable estimates (i.e. returning detailed spatial variations) for acoustic impedance and porosity as compared to sparse-spike inversion algorithms. The calibration of these estimates with petrophysical analysis of wireline log data propose an appropriate agreement among them. Importantly, the results obtained in our case study can be applied to similar basins in Asia with 'tight' oil and 'tight' gas accumulations composed of sand-shale intercalations with different thickness and areal distributions.

Keywords: Post-stack inversion; Acoustic impedance; Sparse-spike inversion; Model-based inversion.

1. Introduction

The evaluation of gas resources in prolific hydrocarbon basins depends on the characterisation of key properties of reservoir rocks, required for developmental planning and risk analyses (Torres and Sen, 2004; Karbalaali et al., 2013). Theses analyses chiefly require the integration of seismic and wireline log data. The reflected amplitudes displayed on seismic sections are function of differences in elastic/acoustic impedances of sub-surface rocks, and thus provide a distribution of contrasts between overlying and underlying lithologies (Yilmaz, 2001; Torres and Sen, 2004; Prskalo, 2007; Karbalaali et al., 2013). This band-limited contrast is used in the estimation of reservoir properties and can be further enhanced through deconvolution operations, which comprise what is usually called as 'an inverse problem'.

Seismic inversion is an interpretation technique used to extract physical properties of rocks and fluids from seismic data (Krebs et al., 2009). To an inversion specialist, the most interesting physical property is acoustic impedance, a product of density and velocity contrasts in sub-surface units. Inverted models of impedance are used by interpreters to derive P- and S-wave velocities, density, elastic parameters (i.e. Lame's parameters), brittleness etc., all of which are believed to be sensitive towards fluid characteristics (Clochard et al., 2009; Alves et al., 2014; Chatterjee et al., 2016; Zhang et al., 2017). Inverted seismic volumes can be processed further using multivariate statistical models to estimate reservoir characteristics such as sand/shale ratios, porosity and water/gas saturations (Hampson et al., 2001; Leiphart and Hart, 2001; Walls et al., 2002; Pramanik et al., 2004; Calderon and Castagna, 2007; Clochard et al., 2009; Singha and Chatterjee, 2014; Singha et al., 2014; Maurya and Sing, 2015; Kumar et al., 2016). Post-stack inversion techniques can also be used to identify reflection events associated with particular depositional geometries (Huuse and Feary, 2005). Some recent studies demonstrated the successful application of post-stack seismic inversion in deep-water seismic data sets (Kumar et al., 2016) and in gas-hydrate estimation (Chatterjee et al., 2016). This makes inversion techniques one of the most widely used interpretational tool in oil and gas exploration.

Seismic inversion has two broad classifications: a) Pre-stack inversion, and b) Post-stack inversion. The interpretation of seismic amplitude variations with offset, i.e. AVO analysis, can be performed on pre-stack data - in which angular information is preserved - to predict lithological and fluid properties (Margrave et al., 1998; Leite and Vidal, 2011). Using well logs, seismic and geologic data, post-stack inversion (at zero offsets) converts seismic data showing

amplitude into a volume of acoustic impedance contrast(s) (Downton, 2005). The final impedance cube can be used to calculate reservoir properties at reservoir scales (Veeken et al., 2004). In detail, post-stack inversion converts the bulk response of seismic waves into acoustic impedance, a property that is intrinsic to the type of rock(s) imaged and facilitates the interpretation of significant geological and petrophysical boundaries in subsurface units (Gambus and Torres, 2008). By reducing any wavelet effects, tuning and side lobes, acoustic impedance will also enhance the resolution of sub-surface layers with recognised hydrocarbon-reservoir potential (Ziolkowski et al., 1998).

The Indus basin has been extensively studied so to evaluate its petroleum elements and associated hydrocarbon potential (Quadri, 1986; Droz and Bellaiche, 1991; Zaigham and Mallick, 2000). A recent study to evaluate the shale gas potential in the lower Indus basin is given by Sheikh and Giao (2017). Here, the Lower Goru formation of Cretaceous age acts as a major reservoir unit and is widely distributed through the lower and middle Indus Basins. Despite its wide spatial distribution, its thickness and reservoir properties are quite heterogeneous. Variations in reservoir properties are mainly attributed to distinct depositional environments in the Cretaceous, shale intercalations and to the style(s) of shale distribution (Ali et al., 2016; Anwer et al., 2017). Multiple studies were carried out to characterise and quantify reservoir properties of the Lower Goru Formation based on petrophysical analysis, rock physics modeling and seismic structural/startigraphic interpretations (Ali et al., 2005; Akhter et al., 2015; Ali et al., 2016; Naeem et al., 2016; Toqeer and Ali, 2017; Anwer et al., 2017; Azeem et al., 2017), but none using different post-stack inversion algorithms tied to a complete borehole data set.

This study focuses on the estimation of reservoir characteristics from post-stack inversion algorithms using 3D seismic and well log data. A 3D seismic cube and well log data from four wells (Sawan-01, Sawan-04, Sawan-05 and Sawan-06) are incorporated in our inversion techniques. The well data comprises gamma ray, resistivity, caliper, density, and sonic logs. The first stage in our analysis consisted of a detailed interpretation of 3D seismic data in order to delineate, mark and map key stratigraphic horizons, subsurface structural and stratigraphic features (Figure 1). The well data was then correlated as a pre-mapping process for locating and tracing the spatial distribution of the reservoir interval (C-sand interval of Lower Goru Formation) in the subsurface (Figure 2). Post-stack inversion algorithms, i.e. model-based and

sparse-spike inversions, were applied to the interpreted data sets to delineate and quantify fluid-rich zones in the Lower Goru Formation, Southern Indus Basin. A further aim was to compare the model-based and sparse-spike inversion algorithms to understand which is the most reliable tool to characterise such formations containing hydrocarbons.

A geo-statistical approach was used in this work to estimate reservoir porosity. Geo-statistical methods use inversion-derived impedance values as an external attribute, while borehole and seismic data are considered as internal attributes (Doyen, 1988). By using a geo-statistical approach in this work, inversion derived impedance was tied to porosity values for C-sands interval of Lower Goru sands in the study area. The complete workflow used for this study is shown in Figure 3.

2. Geological setting

The study area (Sawan) in Figure 4 is a part of Lower Indus basin, the main hydrocarbon-producing basin in Pakistan. The Precambrian basement of the basin has been documented by geophysical surveys and is usually considered as having been tectonically controlled (Balakrishnan, 1977; Farah et al., 1977; Seeber et al., 1980). Numerous structural highs and lows are recognised within this Precambrian basement, and imposed important thickness variations in the overlying sedimentary cover. Amongst these highs, Jacobabad-Khairpur high documented as a horst by Ahmad et al. (2004) is located within our study area (Figure 4). The Jacobabad-Khairpur high divides the Indus basin into the Middle and Lower Indus Basins of Pakistan. Seismic studies reveal that the Sawan area is located on the southeastern flank of Jacobabad-Khairpur high (Ahmad et al., 2004; Abbasi et al., 2016).

Units of the same age as the Lower Goru Formation continue to Iran and India (Alavi, 2004; Raju and Mathur, 2013). In terms of South Asia's hydrocarbon potential, similar basins to the Lower Indus Basin are the Zagros Basin of Iran and multiple sedimentary basins of India. The Zagros Basin is reported as a foreland and foredeep basin containing a variety of oil and gas fields in both carbonate and clastic reservoirs (Alavi, 2004). India also have several basins producing commercial quantity of crude oil and gas, i.e. the Cambay Basin, the Assam shelf Basin, the Mumbai offshore Basin, the Krishna Godavari Basin, and the Rajastan Basin (Klett et al., 2012; Biswas, 1987). Amongst these basins, the Rajastan Basin of India has similar depositional and tectonic histories as those of the southern Indus basin, Pakistan. Similarly,

4

China also has reserves that are hosted in both carbonate and clastic reservoirs of similar nature in different basins, including in the Sichuan, Tarim, and Ordos Basins.

The sedimentary cover above the Precambrian basement is up to 4,000 m thick on the Jaccobabad-Khairpur High, and important volumes of gas are trapped in Jurassic and Cretaceous sandstones, and in Eocene carbonates (Kazmi and Jan, 1997). Based on regional tectono-stratigraphic information, Paleocene clastics (Ranikot Formation) pinch-out towards the Jaccobabad-Khairpur High. This provides evidence for a first Paleogene upflift episode affecting the Jaccobabad-Khairpur High. During the early Eocene, the development of sub-basins and complex basinal paleo-topography is evident due to the presence of carbonate buildups. The basin was then filled with shales during the latter part of the Eocene (Gazih Shale).

The study area shows basement-rooted faults that are mainly oriented in a NNW-SSE direction (Kazmi, 1979; Kazmi and Rana, 1982), and shallower wrench faults cutting through the whole Cretaceous section, terminating at the level of the K-T boundary. These faults may have resulted from transtensional tectonics associated with collision between the Indian and Eurasian plates, followed by anti-clockwise movement of the Indian plate (Kazmi and Jan, 1997).

Peripheral forebulges were formed in paleo-highs during the last episodes of tectonic inversion (Mesozoic and lower Tertiary) in response to crustal and nappe thrusting in the west and northwest parts of the study area. This was the time of the final trap formation, secondary migration of hydrocarbons and reservoir recharging in the Southern Indus Basin (Kadri, 1995; Ahmed et al., 2013). The stratigraphy of the study area includes the Chiltan limestones of Jurassic age at the base (exposed or drilled), overlain by rocks ranging in age from the Cretaceous Sember/Lower Goru Formations to alluvial rocks of Quaternary age (Figure 5).

3. Data and methods

The inversion of seismic data to acoustic impedance has become a standard tool for the prediction of reservoir properties. Relative acoustic impedance inversion helps in the qualitative interpretation of seismic data, while absolute acoustic impedance inversion is essential for the quantitative estimation of reservoir properties. The workflows for both absolute acoustic impedance (model-based inversion) and relative acoustic impedance inversion (sparse-spike inversion) are discussed later in specific sections. In this work, the accuracy of the inversion results was cross-checked by correlating inverted data with borehole petrophysical information.

The following sections give a brief overview of the petrophysical and seismic inversion methods used in this work.

3.1. Petrophysics

The study of rock properties and their interaction with fluids is usually named as petrophysics (Tiab and Donaldson, 2004). The main focus of well-log analysis is to transfer the raw petrophysical data from boreholes into predictable properties of the reservoirs and their fluids (Asquith and Krygowski, 2004). Wireline data are useful in the quantification of porosity, volumes of shale, fluid saturations and permeability of sub-surface reservoirs. Petrophysical evaluations are thus used to identify hydrocarbon-bearing zones within reservoir intervals of distinct geometries. A general workflow for the petrophysical interpretation of hydrocarbon-bearing reservoirs is given in Figure 6.

3.2. Seismic inversion

A brief review of the steps involved in performing seismic inversion is discussed in the following sub-sections.

3.2.1. Wavelet extraction

Seismic inversion is based on the convolution model and states that the synthetic trace, $S(t)$, can be generated from the convolution of Earth's reflectivity series with a desired wavelet (Mallick, 1995; Cooke and Cant, 2010; Barclay et al., 2008), such as:

$$S(t) = W(t) * R + N, \tag{1}$$

where, $W(t)$ is the extracted statistical wavelet, R is reflection co-efficient (RC) series and N is the random noise. A constant phase wavelet, shown in Figure 7, was estimated to perform the correlation of extracted reflectivity and inverted reflectivity from seismic data at well Sawan-05. The window length used in our wavelet extraction ranges from 1600 ms to 2200 ms, with a wavelength of 100 ms. The wavelet extraction algorithm uses seismic data and all available well-log data. To obtain reliable results from seismic interpretation and inversion, the wavelet should be at zero or minimum phase. The amount of phase shift in input wavelet greatly affects the

inversion results. The greater the phase shift, the higher will be the error in the resulting impedance data (Jain, 2013).

3.2.2.Initial Model/Low Frequency (LF) Model

Two terms are used to define acoustic impedance: a) relative acoustic impedance, and b) absolute acoustic impedance. Relative acoustic impedance does not involve the generation of a low frequency model for its calculation. It is a relative layer property and is used in qualitative interpretations. In contrast, absolute acoustic impedance is an absolute layer property and is used in both qualitative and quantitative interpretations (Cooke and Cant, 2010). Absolute acoustic impedance is obtained when a proper low-frequency component (approximately 0-15 Hz) is incorporated in inversion algorithms (Cooke and Cant, 2010). In model-based inversions, low frequencies are added as a part of the inversion algorithm, rather than generating a separate low frequency model. In sparse-spike inversions, the low-frequency model is added separately (Cooke and Schneider, 1983).

A low frequency model generated from the application of a model-based inversion is shown in Figure 8. In order to obtain absolute acoustic impedance from model-based inversion techniques, a low frequency model must be added from the well data to assure more realistic results (Lindseth, 1979). Several authors suggested solutions for building an accurate low frequency model, such as the use of Linear programming algorithms and autoregressive processes in Oldenburg et al. (1983) and generalised linear inversion in Cooke and Schneider (1983). All these approaches face the issue of non-uniqueness because there is more than one model compatible to seismic response (Gavoti et al., 2012).

3.2.3. A priori or low impedance model

To generate *a priori* (or low impedance) models, the input seismic data is modeled by constrained sparse-spike algorithms. This is achieved by convolving the seismic wavelet from the inverted reflectivity series within a defined range of acoustic impedance. This procedure can be accomplished by interpolating (using interpolation algorithms such as trigonometric interpolation, inverse distance weighted methods, and kriging interpolation, etc.) and extrapolating all available information, namely impedance logs and interpreted horizons. Finally

the low-frequency model is added to inverted cube to obtain a better resolution of inversion results. The acoustic impedance cube is then calibrated with rock properties (Ibrahim, 2007). A low impedance model generated for the application of sparse-spike inversion in this work is presented in Figure 9.

3.2.4. Model-based Inversion Theory

A generalised linear inversion algorithm is used in model-based inversions. This algorithm assumes that the seismic trace, $S(t)$, and the wavelet, $W(t)$, are known by the interpreters, and tries to alter the initial guess model until the calculated trace matches with the actual trace to an acceptable level (Gavotti et al., 2012, 2013). In other words, the geological model is altered until the error between the synthetic and original seismic traces is minimised. The basic approach used in the inversion algorithm is, therefore, to solve the function given in Equation 2 and to measure any misfits between real and synthetic data (Gavotti et al., 2013):

$$J = \text{weight}_1 \text{x}(S - W * R) + \text{weight}_2 \text{x}(M - H * R), \qquad (2)$$

where, S is the actual seismic trace, W is the extracted statistical wavelet, R is RC series, M is the initial guess model or interpreted horizon data, and H defines the integration operator, which is convolved with final reflectivity to produce the final impedance. In Equation 2, the first part models the seismic trace while the second part models the impedance initially estimated. Well data is used to control the small amounts of noise, or modeling errors. The workflow for model-based inversions is shown in Figure 10.

3.2.5. Sparse-spike Inversion (SSI)

In this study, we use the Linear Programming (LP) based sparse-spike impedance inversion technique described in Li (2001). The ultimate objective of impedance inversion is to build a bulk model as a series of reflection coefficients. For this purpose, seismic data $x(t)$ and a source wavelet are used as inputs and acoustic impedance (AI) is estimated from that model (Ontiveros

et al., 2014). The relationship between data vector $d = (x_1, x_2, \ldots, x_n)$, model $m = (r_1, r_2, \ldots, r_n)$ and noise "n" is given by Equation 3:

$$Lm + n = d, \tag{3}$$

where, L is the operator that measures the misfit between data and the model. For a given data d, the model vector m can be defined with a probability $p(m|d)$, and can be described by Bayes' formula, shown in Equation 4:

$$p(m|d) = \frac{p(d|m)\, p(m)}{p(d)}, \tag{4}$$

where, $p(m)$ is the *a priori* knowledge on the model and $p(d)$ is *a priori* knowledge on data. Whereas, $p(d|m)$ links the model and the observations. Thus, the *a priori* model is the additional information that comes from well-log data and is used to measure the difference among seismic and synthetic traces (Li, 2002; Ali and Jakobsen, 2011a, b; Ali and Jakobsen, 2014; Anwer et al., 2017). For a model that is based on probability ($p(m|d)$), one may obtain a Maximum-a-Posteriori solution (Ali and Jakobsen, 2011a, b; Ali and Jakobsen, 2014; Anwer et al., 2017). The objective function J for minimization can be written as shown in Equation 5:

$$J = -\log p(m|d) = -\log p(d|m) - \log p(m). \tag{5}$$

As $\log p(d)$ is a constant term, it can be ignored. A solution, in least square sense, can be obtained by maximizing the objective function J which honors an input of *a priori* model (Ontiveros et al., 2014). The workflow followed for LP sparse-spike inversion is shown in Figure 11.

3.2.6   *Geostatistical analysis*

9

Geostatistical techniques are used to link the spatial distribution of rock properties (i.e. petrophysical and petroelastic) to seismic data (Doyen, 1988; Haas and Dubrule, 1994). Geo-statistical methods are routinely used for predicting relation between various petrophysical parameters derived from both well log and seismic data (Doyen, 1988). In these predictions, a statistical relationship is developed between log data and seismic derived properties using a linear regression. This relationship is used to quantify porosity (reservoir character) on the whole seismic cube. The estimated porosities are then correlated with those estimated inside the borehole for reliability check.

4. Results

4.1 Petrophysics

Well log analysis is a fundamental tool providing initial insights towards subsurface geological conditions and reservoir characteristics. On wireline logs, potential gas zones can be identified by low-medium values of gamma ray logs, negative values of spontaneous potential log, high resistivity response, low density response, low neutron porosity values and high acoustic slowness (i.e low velocity) values in sonic logs as compared to surrounding rocks. The petrophysical properties of C-sand interval reservoir are delineated from available wireline logs in Sawan-05, as shown in Figure 12. Table 1 shows the various calculated parameters from the suite of well log data available.

In this well, the C-sand interval reservoir is encountered at a depth of 3255 m having a gross thickness of about 49 m. Based on our petrophysical analysis a 30 m thick net pay zone of clean sand, at a depth range from 3260-3290 m, can be delineated. This sandy zone exhibits a smaller percentage of shale volume (35%), higher effective porosity (19%) and an economic percentage of pore filled hydrocarbons (60%). This highly porous (total porosity 21%) thick pay zone has a substantial hydrocarbon saturation and qualifies as an excellent reservoir (Rider, 2002). Furthermore, the calculated permeability from wireline log data within this reservoir zone lies within a favourable range (Table 1).

4.2 Seismic inversion

The pre-inversion steps adopted in this work involved wavelet extraction and the generation of synthetic seismogram. The wavelet is extracted from seismic data within a specified time window, and including the inline and cross line traces. The extracted wavelet was convolved with reflectivity series, derived from sonic and density logs at well Sawan-05, in order to generate a synthetic seismogram. The synthetic seismogram and seismic traces at well Sawan-05 were correlated as shown in Figure 13. Model-Based and Sparse-spike based inversions were applied on seismic data of Sawan area. The results obtained from both models are discussed separately as follows.

4.2.1 Model-based inversion

A statistical wavelet was extracted in a time window spanning from 1600 ms to 2200 ms within the context of a model-based seismic inversion. The extracted zero phase wavelet (Figure 7) has sharp peak amplitude with higher dominant frequency and minimum side lobes. The frequency and phase spectra are also shown in Figure 7. Figure 14 shows the tie between well log and seismic derived acoustic impedances at Sawan-05. Within the C-sand interval log derived acrostic impedance (blue line), and inverted (seismic) acoustic impedance (red line), are in very good agreement. The comparison of synthetic seismic traces obtained after convolving the final extracted wavelet with the seismic traces at Sawan-05 also result in a excellent correlation (correlation coefficient = 0.99) with a least significant Root Mean Square (RMS) error (0.04 or 502 (m/s)·(g/cc) in terms of impedance).

Figure 15 shows the result of model-based inversion applied to inline 501 in the interpreted 3D seismic volume. The model-based inversion technique is successful in capturing the lateral variations in acoustic impedances by incorporating spatially constant low frequency model (Figure 8). The intended zone of interest, the C-sand interval of the Lower Goru Formation starting at 2160 ms, has low impedance. This low impedance (9394-10024 (m/s)·(g/cc)) is indicative of a gas saturated zone at this particular level (Figure 15). Furthermore, the pattern of

high impedance contrast (between purple, light blue and dominant cyan lines) observed in Figure 15 also indicate this zone as being gas saturated.

The overlying purple-blue layer above the low impedance layer in Figure 15 shows high impedance (10968-11178 (m/s)·(g/cc)), which is believed to reflect the seal unit (D-interval) above the C-sand interval reservoir. Moreover, the low impedance layer at 2160 ms shows a lateral pinch-out towards the northwest (Figure 15). This shows that the thickness of the C-sand interval decreases towards the NW part of the seismic volume. An alternated pattern of medium and high impedance layers (purple, dominant blue and cyan) is observed in the selected time window, a character due to the alternate sand-shale layering present in the Lower Goru Formation at this location.

4.2.2 Sparse-spike inversion

For the sparse-spike inversion, a statistical wavelet was extracted in a time window spanning from 1600 ms to 2200 ms, and its frequency range was adjusted by comparing the inverted trace at well Sawan-05 with the calculated trace. The correlation between synthetic (red) and seismic trace (black) is excellent with a high correlation coefficient (0.99) as shown in Figure 16. The estimated RMS error between the synthetic and seismic trace is 0.04 or 504 (m/s)·(g/cc) in terms of impedance. The results of the sparse-spike inversion applied to inline 501 are shown in Figure 17. The low impedance value, in light-blue colour, is observed at a two-way depth of 2160 ms, which corresponds to the C-sand interval. The impedance ranges from 9500-10000 (m/s)·(g/cc) for this layer. Above this light-blue layer, a high impedance layer is identified as comprising the D-interval (seal unit). The impedance value for this dark-blue layer is >15000 (m/s).(g/cc), and the impedance log also shows a positive peak - indicating a high value for impedance. The high impedance contrast (blue-red colour contrast) observed at places (near well Sawan-05) is due to the presence of a gas saturated zone in the C-sand interval. According to Ibrahim (2007), gas reservoirs are characterised by low acoustic impedance. The impedance values for a good quality gas reservoir range from 8000 to 10000 (m/s)*(g/cc). The high impedance values are, therefore, reflecting the presence of shale. Overall, the lateral resolution of impedance estimated from sparse-spike inversion is low.

4.3 Reservior character (porosity) estimation

Figure 18 shows the cross plot of acoustic impedance and the porosity. The correlation coefficient is reasonably good. A linear regression technique is used to find the correlation coefficient. One can forcefully fit the data through the application of a higher order polynomial, splines and other mathematical techniques. We are not seeking in this work a mere fit but, instead, the recognition of geologically interpretable entities. Since the relation between acoustic impedance and estimated porosity is linear in nature, we therefore used a linear regression technique. Furthermore, it can be argued that this linear relation is valid within the resolution boundaries of seismic and well log data. A higher order polynomial fit will be impossible to interpret and therefore meaningless/misleading in this particular scenario. Henceforth, the porosity estimation from the inverted acoustic impedance is fairly reasonable and realistic within this particular geological settings.

As impedance decreases with increasing in porosity values, we have a linear relationship between porosity and acoustic impedance with a negative slope. The cross plot between acoustic impedance and porosity was made by using their average values at the well locations (Sawan-04, Sawan-05 and Sawan-06) shown in Figure 18. The linear relationship developed between acoustic impedance and porosity by a best fit line is given as follows:

$$\varphi = -0.003 * A - 48.63, \tag{6}$$

where, φ is the effective porosity and A is the inverted impedance from model-based inversion.

5. Discussion

5.1 Combining distinct inversion data in the characterisation of gas reservoirs in South Asia

Various studies have been performed in Asia for the delineation of gas reservoirs using seismic post-stack inversion techniques. The study performed by Sinha and Mohanty (2015) is based on post-stack model-based and band limited inversions applied to the Krishna Godavari Basin of India. The Cretaceous sedimentary strata (sand/shale units) of this basin are similar to that of Southern Indus Basin Pakistan (Gupta, 2006). Their study indicates that post-stack inversion gives valuable results in terms of stratigraphic interpretation, reservoir characterisation and demarcation of potential gas saturated zones in the Krishna Godavari Basin of India. The high impedance contrasts offered by inversion are interpreted as free gas saturated zone.

Furthermore, the model-based inversion in this case also provides very-high quality results as compared to band limited inversion. The same results are obtained from inversion techniques in a case study from an oilfield in Persian Gulf, in Iran (Karbalaali et al., 2013). The study of Karbalaali et al. (2013) also comprises a post-stack model-based inversion and crossplots of inverted volumes for the identification of productive hydrocarbon zones. This same study showed that high acoustic impedence contrasts in sand/shale successions (Ghar Formation) are due to saturated hydrocarbon zones.

In this study, the application of both inversion schemes on a 3D seismic cube provide a reasonable estimate of acoustic impedence, which can be linked to spatial lithological variations and use in the delineation of hydrocarbon-bearing zones (gas saturated zone). Here, the sparse-spike inversion algorithm was able to delieneate gas saturated zones, but was unable to capture the lithological variations (lateral pinch-out) of the C-sand reservoir interval. The model-based inversion algorithm was able to capture both lithological and fluid characteristics. Also, the lateral and vertical variations of acoustic impedence for model-based inversion provides a good match with well data as compared to the sparse-spike inversion (this latter with a relative low resolution).

5.2 Importance of geo-statistical analyses in porosity calculations

Porosity and permeability are the most important parameters in reservoir characterisation and are difficult to estimate. The difficulty in estimating porosity and permeability comes from the fact that these parameters vary considerably at reservoir scale and can only be effectively measured at specific well locations. The solution to this caveat requires the integration of rock physics, petrophysics, seismic inversion and surface seismic in order to get more reliable results (Leite and Vidal, 2011).

The quantitative estimation of porosity in reservoir rocks is as difficult as it is important. Further difficulties when evaluating porosity arise when dispersed shale is present in reservoir rocks or the reservoir rock exhibits several types of porosities (Adekanle and Enikanselu, 2013). Porosity can be determined by various methods involving wireline log data, mathematical models and laboratory procedures. Well data provide the best vertical resolution and good estimates of porosity at certain locations within an area of interest. As wells are sparsely located

in the field and it is hard to estimate reservoir parameters (i.e. porosity) between wells, the integration of seismic inversion results with petrophysics is crucial to improve our knowledge of the spatial distribution of porosity. The ultimate goal of seismic inversion is to provide models not only of acoustic impedance but also of other reservoir properties such as effective porosity and water saturation for regions between wells (Rijks and Jauffred, 1991) .

Using equation 6, the inverted impedance surface of the C-sand interval estimated from the model-based post-stack inversion algorithm (Figure 19) was converted into porosity in a second stage (Figure 20). The impedance surface shows that the low impedance value in the C-sand interval follows a SW to NE direction, and that a favourable distribution of porosity is observed in this direction. The porosity varies from 6 % (dark cyan colour) to 32 % (orange colour). Nearer to well Sawan-05, the average porosity is around 19 % (light cyan to green colours). The porosity value estimated at the Sawan-05 well location by petrophysics matches the value estimated from seismic inversion (Figure 20). This study provides guidance towards the assessments of reservoir identification and reservoir properties distribution over the entire reservoir's surface through geo-statistical analysis. It may be considered a useful work to characterise sand-shale reservoirs in South Pakistan, and in other basins of Asia as suggested in section 2.

6. Conclusions

The integration of petrophysics, geostatistical analysis and model-based inverted acoustic impedance can result in an effective estimation of reservoir character. In this study, two types of inversion algorithms are applied and compared to delineate reservoir character in the Sawan area, Lower Indus Basin, Pakistan. Sparse-spike inversion clearly delineates the reservoir zone, but fails to map detailed spatial variations. On the other hand, the model-based inversion successfully captured the detailed spatial/lithological variations (in high resolution) within the reservoir zone – it is therefore preferred over the sparse-spike inversion. Spatial distribution of inversion-based (estimated) porosity within the C-sand interval ranges from 6% to 32%. In well Sawan-05, the estimated porosity for C-sand interval is around 19%. Furthermore, the porosity obtained from post-stack inversion and petrophysical analyses of the well Sawan-05 is in best agreement. This methodology of reservoir characterization can be implemented to other basins in Asia with similar geological settings.

Acknowledgements

REFERENCES

- Abbasi, S.A., Kalwar, Z., Solangi, S.H., 2016. Study of Structural Styles and Hydrocarbon Potential of RajanPur Area, Middle Indus Basin, Pakistan. BU. J. ES, 1(1), 36-41.

- Adekanle, A., Enikanselu, P.A.., 2013. Porosity Prediction from Seismic Inversion Properties over 'XLD' Field, Niger Delta. Am. J. Sci. Ind. Re, 4(1), 31-35. DOI: 10.5251/ajsir.2013.4.1.31.35.

- Ahmad, N., Fink, P., Sturrock, S., Mahmood, T., Ibrahim, M., 2004. Sequence Stratigraphy as Predictive Tool in Lower Goru Fairway, Lower and Middle Indus Platform, Pakistan. PAPG, ATC. 85-104.

- Ahmed, W., Azeem, A., Abid, M.F., Rasheed, A., and Aziz, K.., 2013. Mesozoic Structural Architecture of the Middle Indus Basin, Pakistan—Controls and Implications. PAPG/SPE Ann. Tech. Conf, Islamabad, Pakistan. 1-13.

- Akhter, G., Ahmed, Z., Ishaq, A., Ali, A., 2015. Integrated interpretation with Gassmann fluid substitution for optimum field development of Sanghar area, Pakistan: a case study. Arab. J. Geosci, 8(9), 7467-7479. DOI: 10.1007/s12517-014-1664-8.

- Alavi, M., 2004. Regional stratigraphy of the Zagros fold-thrust belt of Iran and its pro-foreland evolution. Am J. Sci. 304(1), 1-20. DOI: 10.2475/ajs.304.1.1.

- Ali, A., Ahmad, Z., Akhtar, G., 2005. Structural interpretation of seismic profiles integrated with reservoir characteristics of Qadirpur area. Pak. J. of Hydrocarb. Res, 15, 25-34.

- Ali, A., Hussain, M., Rehman, K., Toqeer, M., 2016. Effect of Shale Distribution on Hydrocarbon Sands Integrated with Anisotropic Rock Physics for AVA Modelling: A Case Study. Act. Geophys, 64(4), 1139-1163.

- Ali, A., Jakobsen, M., 2011a. On the accuracy of Rüger's approximation for reflection coefficients in HTI media: implications for the determination of fracture density and orientation from seismic AVAZ data. J. Geophy. Eng, 8, 372-393.

- Ali, A., Jakobsen, M., 2011b. Seismic characterization of reservoirs with multiple fractures sets using velocity and attenuation anisotropy data. J. Appl. Geophy, 75, 590-602. 10.3997/2214-4609.20149364

- Ali, A., Jakobsen, M., 2014. Anisotropic permeability in fractured reservoirs from frequency-dependent seismic Amplitude Versus Angle and Azimuth data. Geophy. prospect, 62(2), pp.293-314. DOI: 10.1111/1365-2478.12084.

- Alves, T.M., Kurtev, K., Moore, G.F., Strasser, M., 2014. Assessing the internal character, reservoir potential, and seal competence of mass-transport deposits using seismic texture: A geophysical and petrophysical approach. AAPG Bulletin, 98(4), 793-824. DOI:10.1306/09121313117.

- Anwer, H.M., Alves, T.M., Ali, A., Zubair., 2017. Effects of sand-shale anisotropy on amplitude variation with angle (AVA) modelling: The Sawan Gas Field (Pakistan) as a key case-study for South Asia's sedimentary basins, J. Asian Earth Sci, DOI:10.1016/j.jseaes.2017.07.047.

- Asquith, G.B., Krygowski, D., Gibson, C.R., 2004. Basic well log analysis.Tulsa: AAPG. 16, pp.244.

- Azeem, T., Chun, W., Khalid, P., Qing, L., 2017. An integrated petrophysical and rock physics analysis to improve reservoir characterization of Cretaceous sand intervals in Middle Indus Basin, Pakistan. J. Geophy. Eng, 14(2), 212.

- Balakrishnan, T.S., 1977. Role of geophysics in the study of geology and tectonics. Geophysical case histories of India. AEG. 1,9-27.

- Barclay, F., Bruun, A., Rasmussen, K.B., Alfaro, J.C., Cooke, A., Cooke, D., Salter, D., Godfrey, R., Lowden, D., McHugo, S., 2008. Özdemir H. Seismic inversion: Reading between the lines. Oilfield Review. 20(1): 42-63.

- Biswas, S.K., 1987. Regional tectonic framework, structure and evolution of the western marginal basins of India. Tectonophy, 135(4), 307-327. DOI: 10.1016/0040-1951(87)90115-6.

- Calderon, J.E., Castagna, J.P., 2007. Porosity and lithology estimation using rock physics and multi-attribute transforms in Balcon field, Colombia. Lead. Edge 26, 142-150.

- Chatterjee, R., Singha, D., Ojha, M., Sen, M., 2016. Porosity estimation from pre-stack seismic data in gas-hydrate bearing sediments, Krishna-Godavari basin, India. J. Nat. Gas Sci. Eng, 33, 562-572. DOI: 10.1016/j.jngse.2016.05.066

- Clochard, V., Delépine, N., Labat, K., Ricarte, P., 2009. Post-stack versus pre-stack stratigraphic inversion for CO_2 monitoring purposes: A case study for the saline aquifer of the Sleipner field. In SEG Technical Program Expanded Abstracts. 2417-2421.

- Cooke, D.A., Schneider, W.A., 1983. Generalized linear inversion of reflection seismic data. Geophy. 48(6), 665-676. DOI.org/10.1190/1.1441497.

- Cooke, D., Cant, J., 2010. Model-based Seismic Inversion: Comparing deterministic and probabilistic approaches. CSEG Recorder. 35(4), 28-39.

- Downton, J.E., 2005. Seismic parameter estimation from AVO inversion. Ph.D. Dissertation. UOC.

- Doyen, P.M., 1988. Porosity from seismic data: A geostatistical approach. Geophy, 53(10), 1263-1275. DOI.org/10.1190/1.1442404

- Droz, L., Bellaiche, G., 1991. Seismic facies and geologic evolution of the central portion of the Indus Fan. In Seismic facies and sedimentary processes of submarine fans and turbidite systems (pp. 383-402). Springer New York.

- Gambús-Ordaz, M.,Torres-Verdín, C., 2008. A study to assess the value of post-stack seismic amplitude data in forecasting fluid production from a Gulf of Mexico reservoir. J. Pet. Sci. Eng, 62(1), 1-15. DOI.org/10.1016/j.petrol.2008.06.001.

- Gupta, S.K., 2006. Basin architecture and petroleum system of Krishna Godavari Basin, east coast of India. The Leading Edge. 25(7), 830-7. DOI.org/10.1190/1.2221360.

- Farah, A., Mirza, M.A., Ahmad, M.A., and Butt, M.H., 1977. Gravity field of the buried shield in the Punjab plain, Pakistan. Bull. Geol. Soc. Amer, 88 (8), 1147-1155. DOI: 10.1130/0016-7606(1977)88.

- Gavotti, P.E., Lawton, D.C., Margrave, G.F., Isaac, J.H., 2012. Post-stack inversion of the Hussar low frequency seismic data. In CREWES Research Report. 24, 1-22.

- Gavotti, P., Lawton, D.C., Margrave, G., Isaac, J.H., 2013, June. Model-Based Inversion of Low-Frequency Seismic Data. In 75th EAGE Conference and Exhibition incorporating SPE EUROPEC 2013. DOI: 10.3997/2214-4609.20130047.

- Haas, A., Dubrule, O., 1994. Geo-statistical inversion a sequential method of stochastic reservoir modelling constrained by seismic data. First break. 12(11), 561-569. DOI: 10.3997/1365-2397.1994034

- Hampson, D., Schuelke, J., Quirein, J., 2001. Use of multi-attribute transforms to predict log properties from seismic data. Geophy, 66, 220-236. DOI.org/10.1190/1.1444899.

- Huuse, M., Feary, D., 2005. Seismic inversion for acoustic impedance and porosity of Cenozoic cool-water carbonates on the upper continental slope of the Great Australian Bight. Mar. Geol, 215(3), 123-134. DOI: 10.1016/j.margeo.2004.12.005

- Ibrahim, M., 2007. Seismic inversion Data, A tool for reservoir characterization/Modeling Sawan Gas Field - A case study, PAPG, ATC.

- Jain, C., 2013. Effect of seismic wavelet phase on post stack inversion. 10th Biennial Int. Conf. exp. P-410. Kadri, I.B., 1995. Pet. Geol. Pak, PPL.

- Karbalaali, H., Shadizadeh, S. R., Riahi, M. A., 2013. Delineating Hydrocarbon Bearing Zones Using Elastic Impedance Inversion: A Persian Gulf Example. Iran. J. Oil. Gas. Sci. Tech, 2(2), 8-19. DOI: 10.22050/IJOGST.2013.3534

- Kazmi, A.H.,1979. Active fault system in Pakistan. In: Farah A, and DeJong KA (eds.) Geodynamics of Pakistan. Geol. Sur. Pak, Quetta. 285-294.

- Kazmi, A.H., Jan, M.Q., 1997. Geology and Tectonics of Pakistan. Graphic Publishers, Karachi, Pakistan.

- Kazmi, A.H., Rana, R.A., 1982. Tectonic map of Pakistan. Geol. Sur. Pak, Quetta. Scale 1:2.000.000.

- Klett, T.R., Schenk, C.J., Wandrey, C.J., Brownfield, M., Charpentier, R.R., Cook, T., Gautier, D.L., Pollastro, R.M., 2012. Assessment of Potential Shale Gas Resources of the Bombay, Cauvery, and Krishna–Godavari Provinces, India, USGS Fact Sheet 2011-3131. (2 pp.).

- Krebs, J.R., Anderson, J.E., Hinkley, D., Neelamani, R., Lee, S., Baumstein, A., Lacasse, M.D., 2009. Fast full-wave field seismic inversion using encoded sources. Geophys, 74(6), WCC177-WCC188. DOI.org/10.1190/1.3230502

- Kumar, R., Das, B., Chatterjee, R., Sain, K., 2016. A methodology of porosity estimation from inversion of post-stack seismic data. J. Nat. Gas Sci. Eng, 28, 356-364. DOI: 10.1016/j.jngse.2015.12.028.

- Leiphart, D.J., Hart, B.S., 2001. Comparison of linear regression and a probabilistic neural network to predict porosity from 3D seismic attributes in lower Brushy Canyon channeled sandstones, southeast New Mexico. Geophy, 66, 1349-1358. DOI.org/10.1190/1.1487080

- Leite, E.P., and Vidal, A.C., 2011. 3D porosity prediction from seismic inversion and neural networks. Comp. Geosci, 37(8), 1174-1180. DOI:10.1016/j.cageo.2010.08.001.

- Li, Q., 2001. LP sparse-spike inversion, Strata Technique Document, HRSS Ltd.

- Li, Q., 2002. Sparse-spike inversion and resolution limit. CSEG Geophy.

- Lindseth, R.O., 1979. Synthetic sonic logs – a process for stratigraphic interpretation: Geophysics. 44, p. 3-26. DOI.org/10.1190/1.1440922.

- Mallick, S., 1995. Model-based inversion of amplitude-variations-with-offset data using a genetic algorithm. Geophy, 60(4), 939-954. DOI.org/10.1190/1.1443860.

- Margrave, G.F., Lawton, D.C., Stewart, R.R., 1998. Interpreting channel sands with 3c-3d seismic data. The Leading Edge. 17(4),509-513. DOI.org/10.1190/1.1438000.

- Maurya, S., Singh, K., 2015. Reservoir characterization using model-based inversion and probabilistic neural network. In 1st int. conf. on recent trend in eng. and Tech.

- Naeem, M., Jafri, M., Moustafa, S., AL-Arifi, N., 2016. Seismic and well log driven structural and petrophysical analysis of the Lower Goru Formation in the Lower Indus Basin, Pakistan. Geosci. J, 20(1), 57-75.

- Oldenburg, D.W., Scheuer, T., Levy, S., 1983. Recovery of the acoustic impedance from reflection seismograms. Geophy, 48(10), 1318-1337. DOI.org/10.1190/1.1441413.

- Ontiveros, T., Herrera, V., Meza, R., 2014. Seismic Inversion Applied To Geological And Operational Monitoring Of Drilling Horizontal Wells. In The Carabobo Area of the Faja Petrolífera Del Orinoco.

- Pramanik, A.G., Singh, V., Vig, R., Srivastava, A.K., Tiwary, D.N., 2004. Estimation of effective porosity using geostatistics and multiattribute transforms: a case study. Geophy, 69, 352-372. DOI.org/10.1190/1.1707054

- Prskalo, S., 2007. Application of Relation between Seismic Amplitude, Velocity and Lithology in Geological Interpretation of Seismic data. J. Hung. Geomath, 2, pp.51-68.

- Quadri, S.V., 1986. Hydrocarbon prospects of southern Indus basin, Pakistan. AAPG Bulletin, 70(6), 730-747.

- Raju, S.V., Mathur, N., 2013. Rajasthan lignite as a source of unconventional oil. Current Science(Bangalore). 104(6), 752-7.

- Rijks, E.J.K., Jauffred, J.C.E.M., 1991. Attribute extraction: An important application in any detailed 3-D interpretation study: The Leading Edge. 10, 11-19. DOI.org/10.1190/1.1436837.

- Rider, M., 2002. The geological interpretation of well logs. 2nd ed. p 291.

- Robinson, E.A., Silvia, M.T., 1978. Digital signal processing and time series analysis. Holden-day.

- Seeber, L., Quittmeyer, R.C.,Armbruster, J.G.,1980. Seismotectonics of Pakistan: A review of results from network data and implications for the Central Himalayas. Geol. Bull. University of Peshawar. 13, 151-168.

- Sheikh, N., Giao, P., 2017. Evaluation of shale gas potential in the Lower Cretaceous Sembar Formation, the Southern Indus Basin, Pakistan. J. Nat. Gas. Sci. Eng, 44, 162-176. DOI: 10.1016/j.jngse.2017.04.014.

- Singha, D.K., Chatterjee, R., 2014. Detection of overpressure zones and a statistical model for pore pressure estimation from well logs in the Krishnae Godavari Basin, India. Geochem. Geophy. Geosystems, 15, 1009-1020. DOI: DOI: 10.1002/2013GC005162.

- Singha, D.K., Chatterjee, R., Sen, M.K., Sain, K., 2014. Pore pressure prediction in gashydrate bearing sediments of Krishnae Godavari Basin in, India. Mar. Geol, 357, 1-11. DOI: 10.1016/j.margeo.2014.07.003.

- Sinha, B., Mohanty, P. R., 2015. Post stack inversion for reservoir characterization of KG basin associated with gas hydrate prospects. J. Ind. Geophys. Union (April 2015). 19(2), 200-204.

- Seeber, L., Quittmeyer, R.C., Armbruster, J.G., 1980. Seismotectonics of Pakistan: A review of results from network data and implications for the Central Himalayas. Geol. Bull. University of Peshawar. 13, 151-168.

- Tiab, D., Donaldson, E.C., 2004. Petrophysics: Theory and Practice of measuring reservoir rock and fluid transport properties. Gulf Prof Pub.

- Toqeer, M., Ali, A., 2017. Rock physics modelling in reservoirs within the context of time lapse seismic using well log data. Geosci. J, 21(1), 111-122.

- Torres, C., Sen, M., 2004. Integrated Approach for the Petrophysical Interpretation of Post- and Pre-stack 3D Seismic Data, Well Log and Core Data, Geological Information and Production Data via Bayesian Stochastic Inversion. 3rd Annual Report, Institute of Geophysics, Texas.

- Veeken, PCH., Da Silva, M., 2004. Seismic inversion methods and some of their constraints. First break. 22(6), 47-70. DOI: 10.3997/1365-2397.2004011.

- Walls, J.D., Taner, M.T., Taylor, G., Smith, M., Carr, M., Derzhi, N., Drummond, J., McGuire, D., Morris, S., Bregar, J., Lakings, J., 2002. Seismic reservoir characterization of a U.S. Midcontinent fluvial system using rock physics, poststack seismic attributes, and neural networks. Lead. Edge 21, 428-436. DOI: doi.org/10.1190/1.1481248.

- Yilmaz, Ö., 2001. Seismic data analysis: Processing, inversion, and interpretation of seismic data. Society of exploration geophysicists.

- Zaigham, N., Mallick, K., 2000. Prospect of hydrocarbon associated with fossil-rift structures of the southern Indus basin, Pakistan. AAPG bulletin, 84(11), 1833-1848. DOI: 10.1306/8626C3A7-173B-11D7-8645000102C1865

- Zhang, S., Huang, H., Dong, Y., Yang, X., Wang, C. and Luo, Y., 2017. Direct estimation of the fluid properties and brittleness via elastic impedance inversion for predicting sweet spots and the fracturing area in the unconventional reservoir. J. Nat. Gas. Sci. Eng,45, 415-427. DOI: 10.1016/j.jngse.2017.04.028.

- Ziolkowski, A., Underhill, J.R., Johnston, R.G., 1998. Wavelets, well ties, and the search for subtle stratigraphic traps. Geophy, 63(1), 297-313. DOI:org/10.1190/1.1444324.

Table 1: Estimated petrophysical properties of the reservoir zone, 3260-3290 m, of the C-sand interval at well Sawan-05.

Petrophysical Property	Shale Volume (V_{sh})	Total Porosity (φ_T)	Effective Porosity (φ_E)	Permeability (K)	Water Saturation (S_w)	Hydrocarbon Saturation (H_w)	Gross Thickness	Net Pay
Units	v/v	v/v	v/v	Milidarcy	v/v	v/v	Meter	Meter
Values	35%	21%	19%	95	40%	60%	28	22
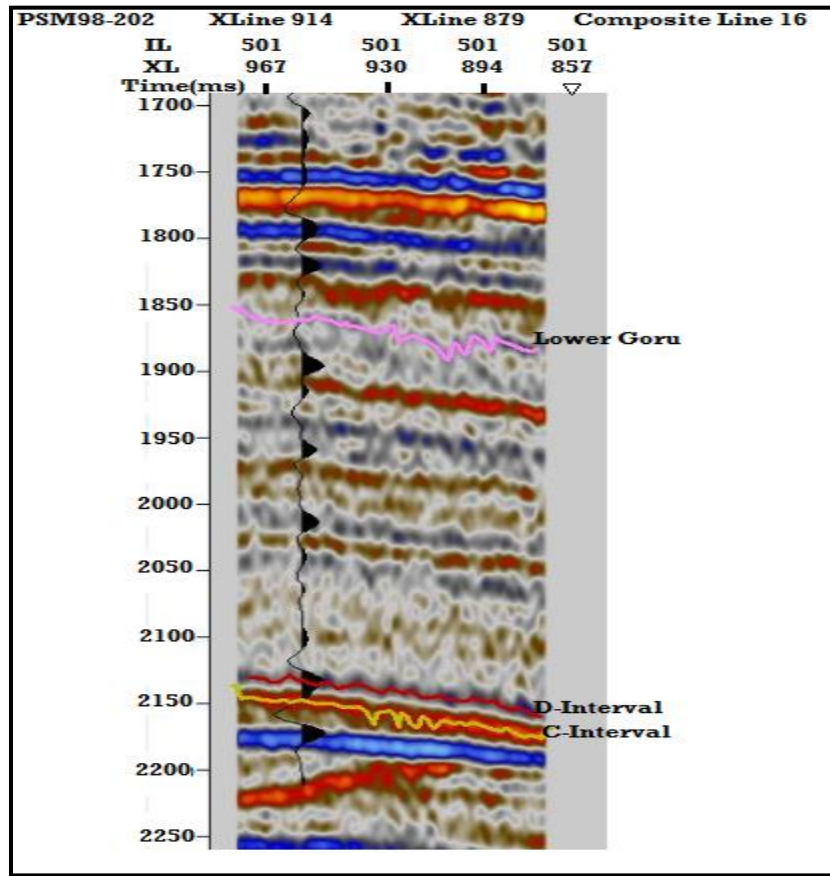
Figure 1: Display of seismic inline 501 highlighting the interpreted reservoir zone. The seismic to well tie (black color wiggle) is also shown using the data of well Sawan-05.
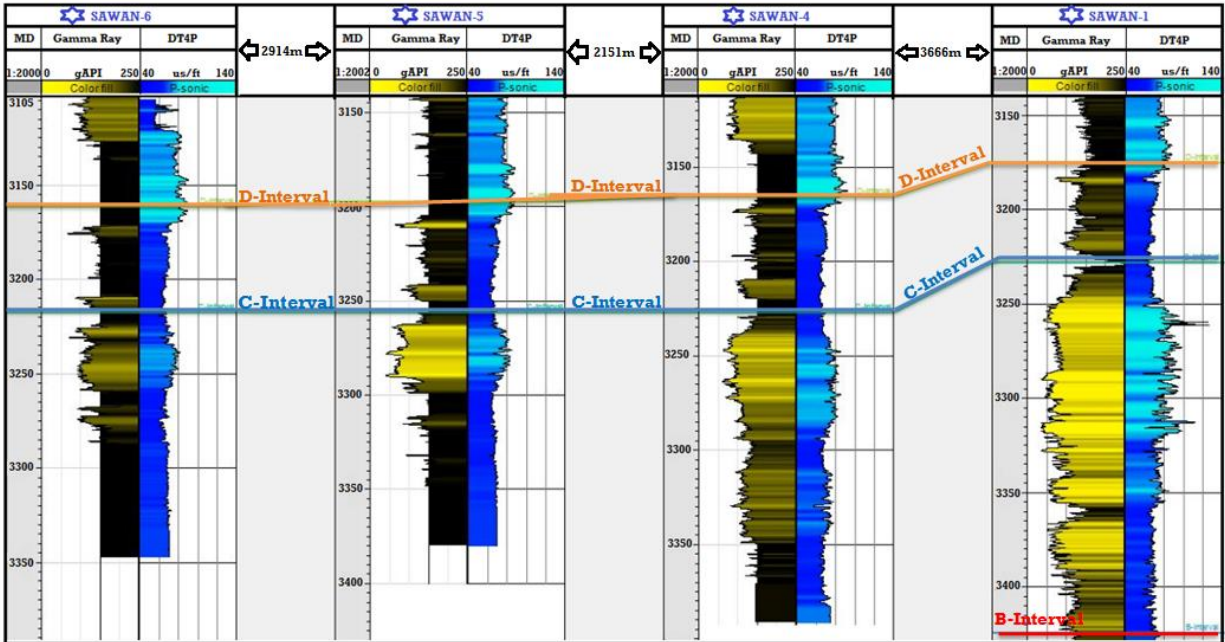
Figure 2: Well correlations based on Gamma ray and sonic (DT) log. The correlation shows the spatial distribution of different sands of Lower Goru Formation. The C-sand interval within the Lower Goru Formation comprises the main reservoir interval in the study area.
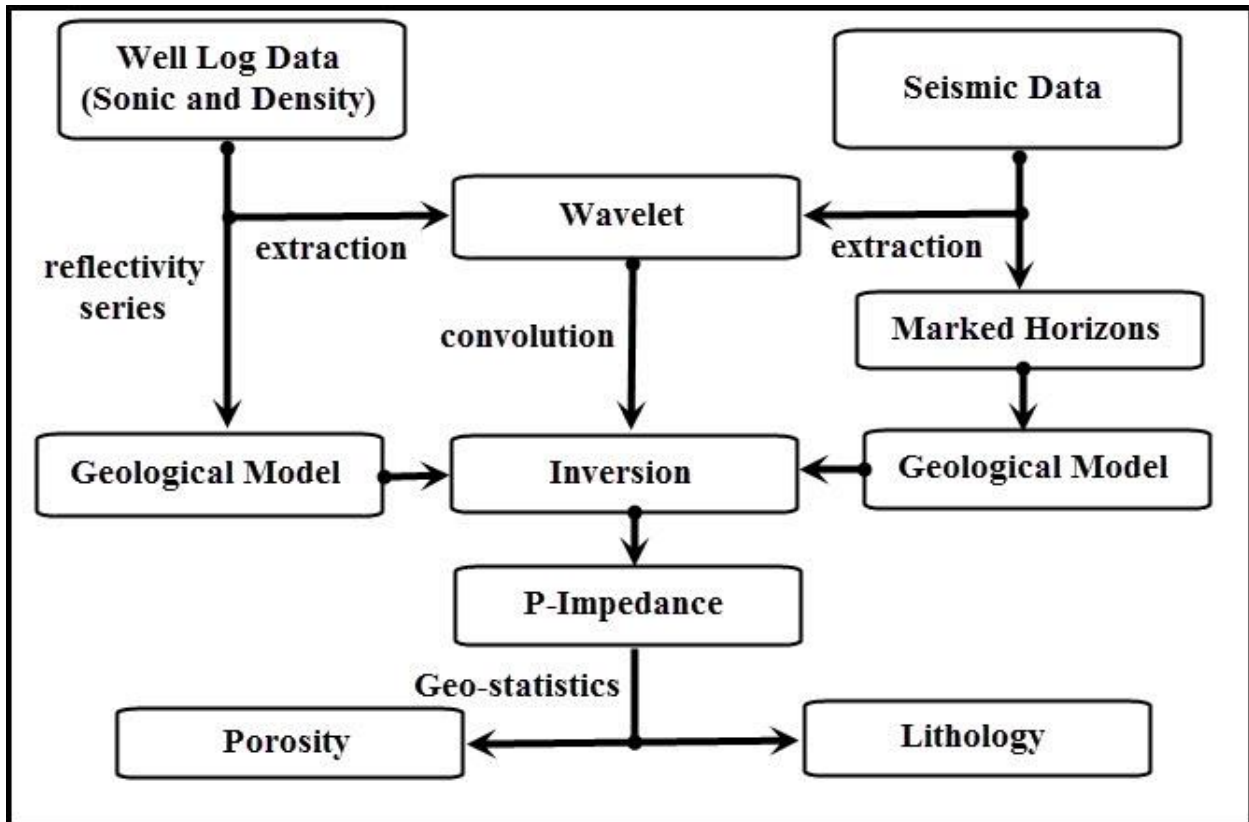
Figure 3: Generalised work flow for seismic post stack inversion.
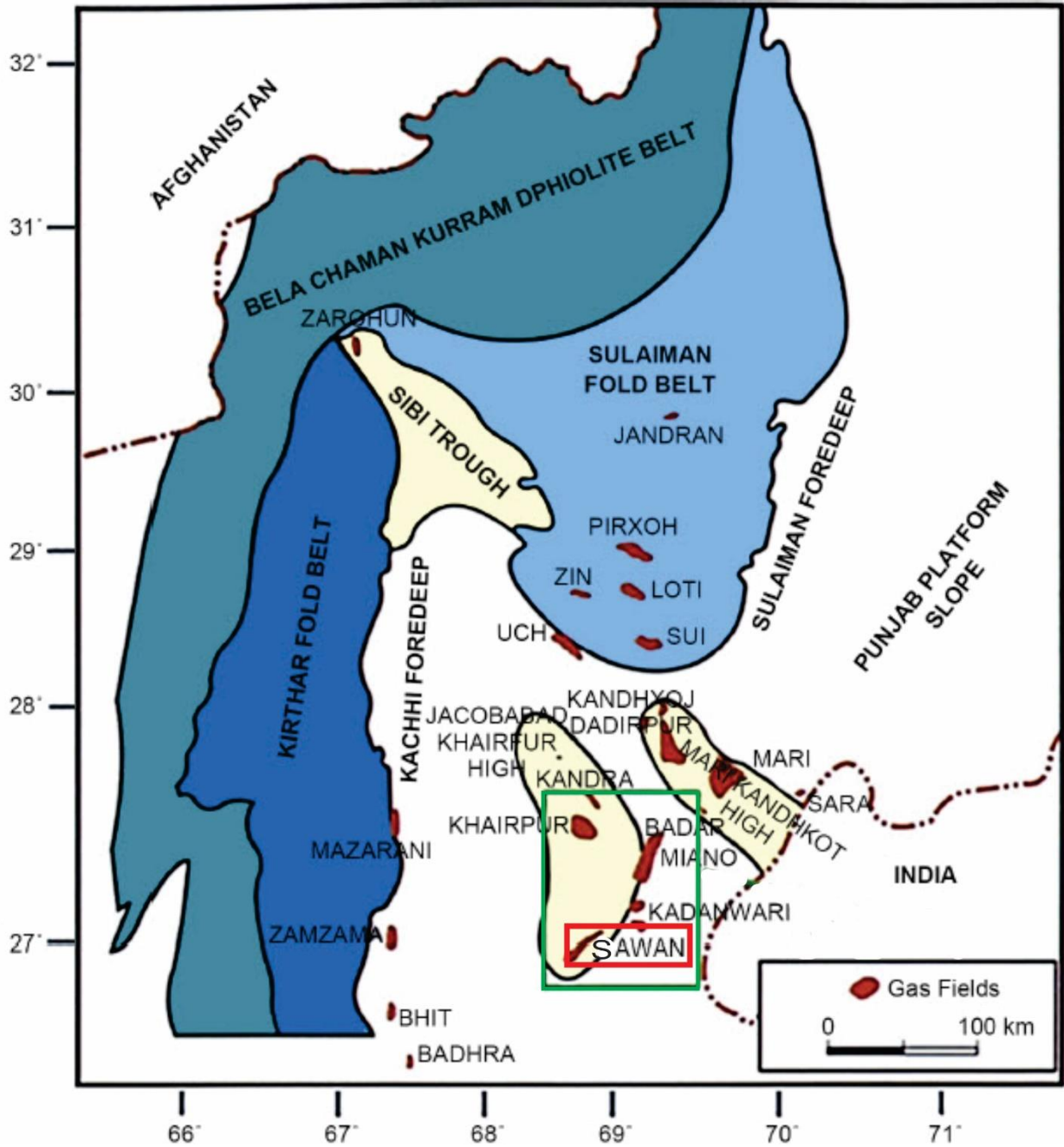
Figure 4: Regional tectonic map and geological boundaries of the study area. The green and red colour rectangles show the locations of the Jacobabad-Khairpur high and the study area, respectively (Ahmad et al., 2013).

Period	Epoch	Formation	Lithology	Desciption
	Quateranry	Aluvium		Sandstone, Clay, Shale and Conlomerate
	Eocene	Kirthar		Limestone and Shale
		Laki		Limestone and Shale
Tertiary	Paleocene	Upper Ranikot		Shale and Sandstone
		Lower Ranikot		
		Parh		Limestone
	Upper	Upper Goru		Shale and Marl (Main Seal)
Cretaceous		Lower Goru		Shale and Sandstone (Main Reservoir and Source)
	Lower	Sember		Shale and Sandstone (Main Source)
JURASSIC	Upper	Chiltan		Limestone

Legend

Shale

Marl

Sandstone

Limestone

Conglomerate

Figure 5: Stratigraphic column for the study area, Lower Indus Basin, Pakistan (Abbasi et al., 2016).
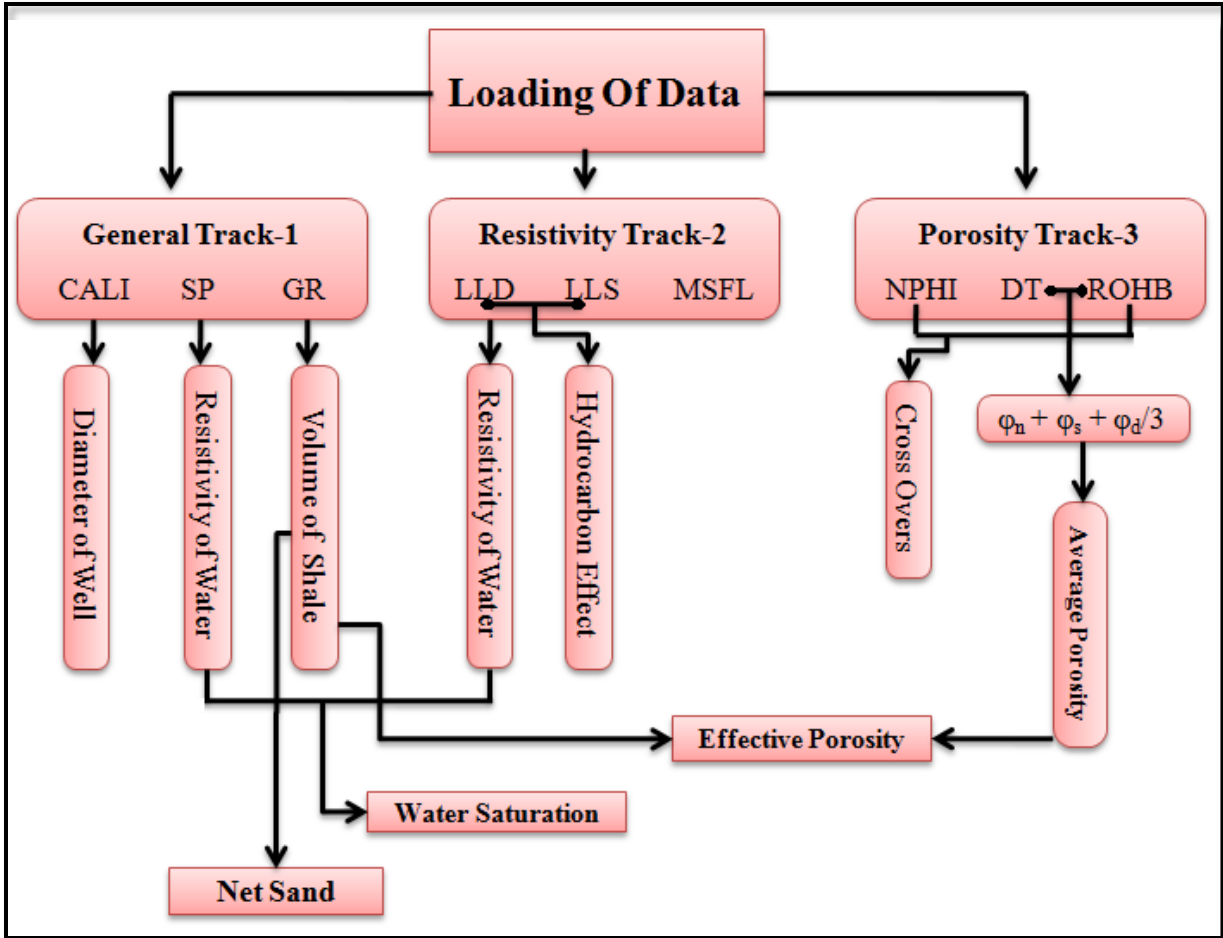
Figure 6: Basic flow diagram for the petrophysical analyses adopted in this study.
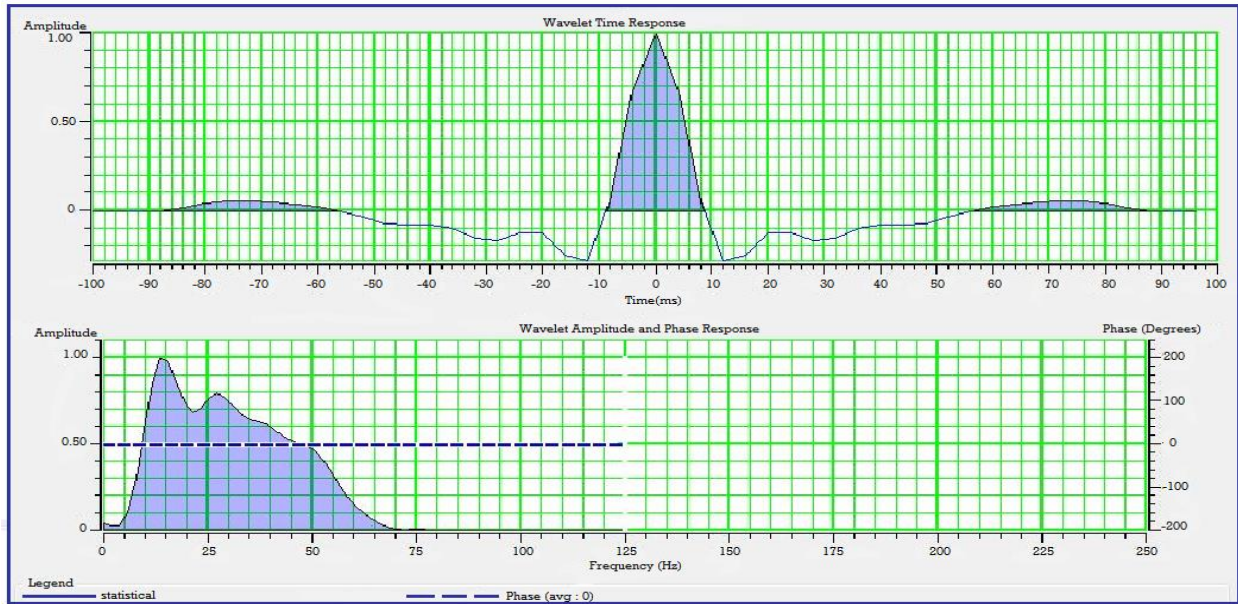
Figure 7: Extracted statistical wavelet from seismic data along with its amplitude and phase spectra. The dotted line displays the average phase of the wavelet.
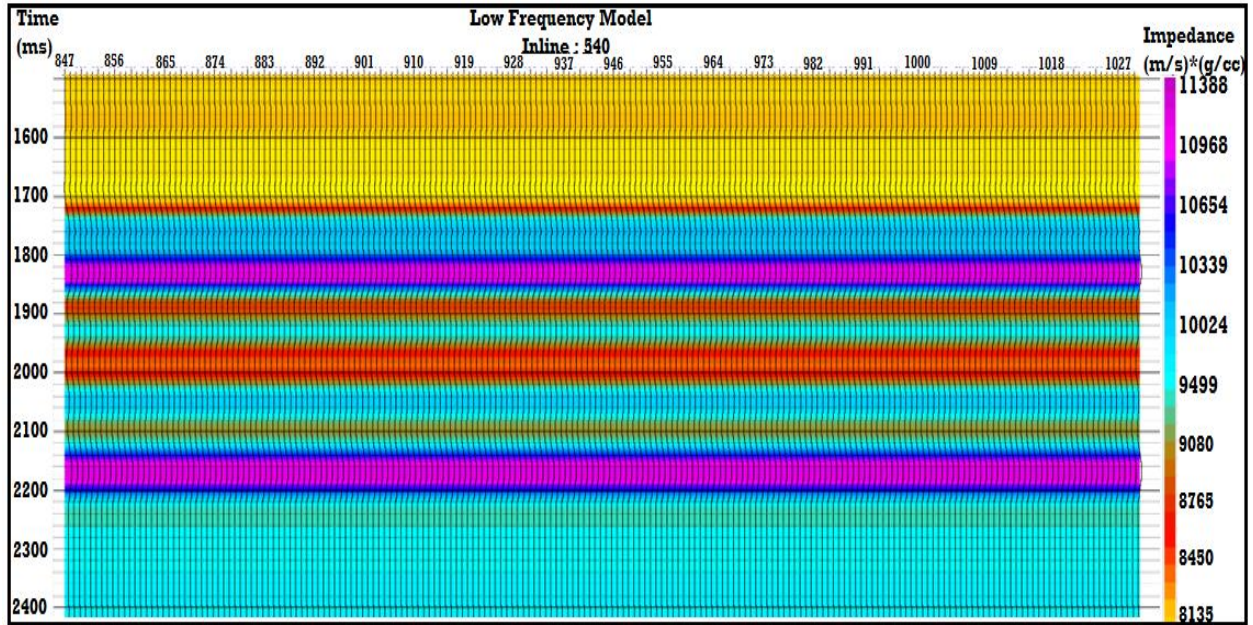
Figure 8: An example of a low frequency model used for the application of the model-based inversion in this study.
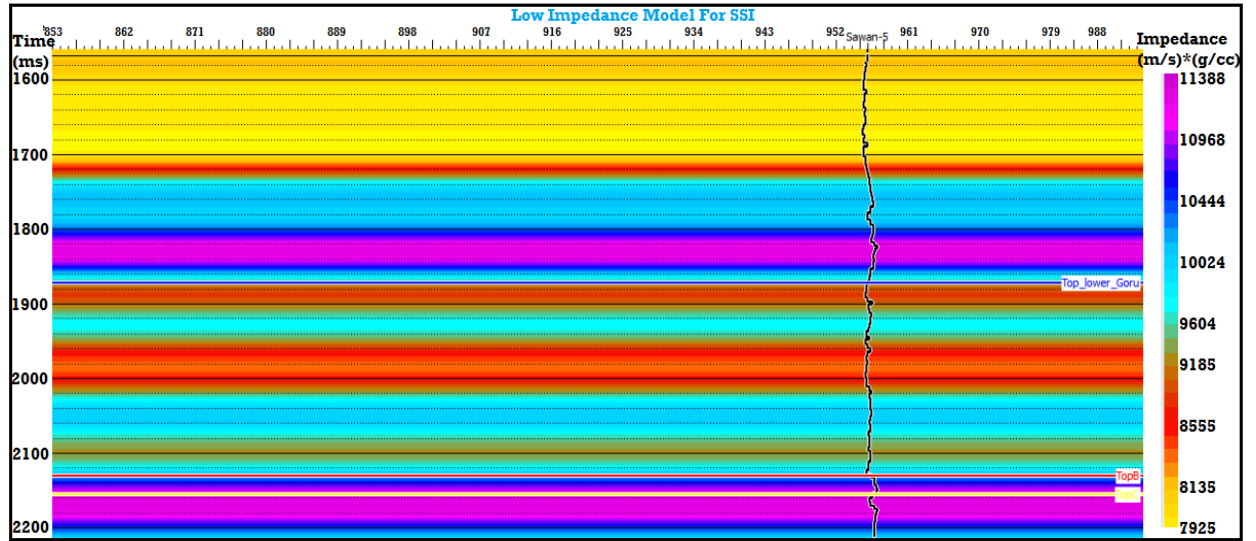
Figure 9: An example of an *a priori* model/low impedance model used for the application of the sparse-spike inversion in this study.
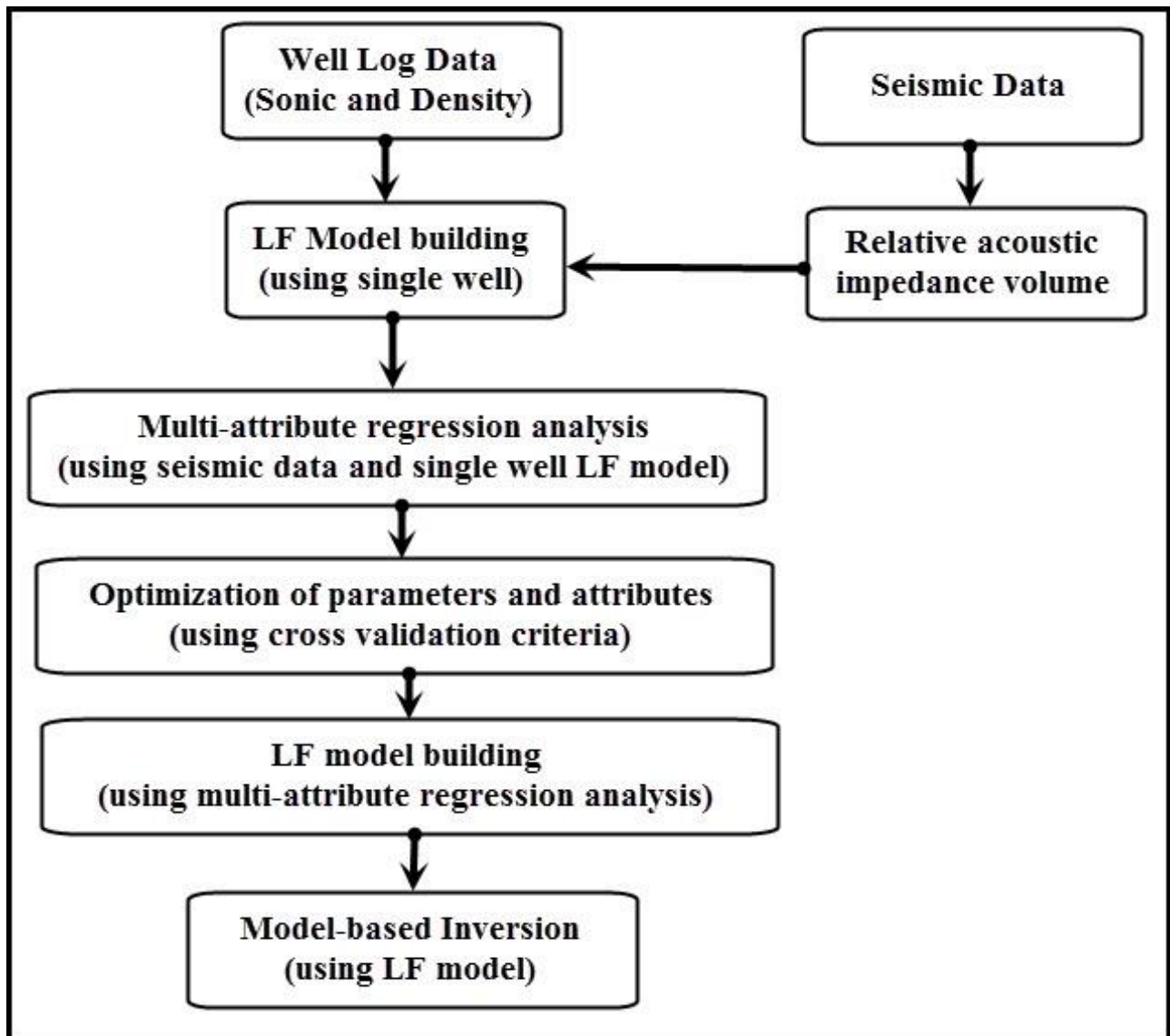
Figure 10: An impedance estimation scheme based on the model-based inversion (Kumar et al., 2016).
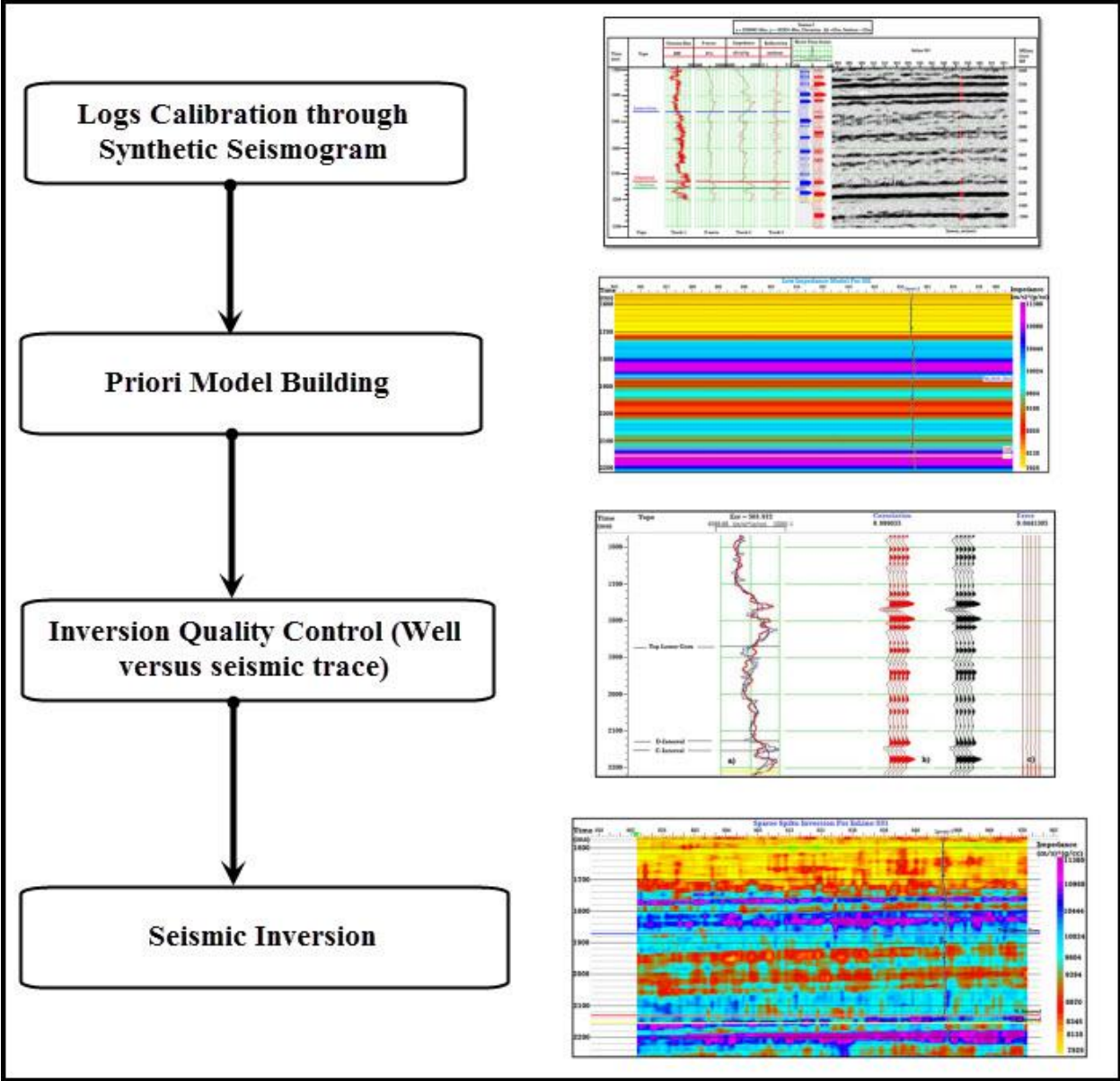
Figure 11: Work flow for the application of a sparse-spike Inversion.
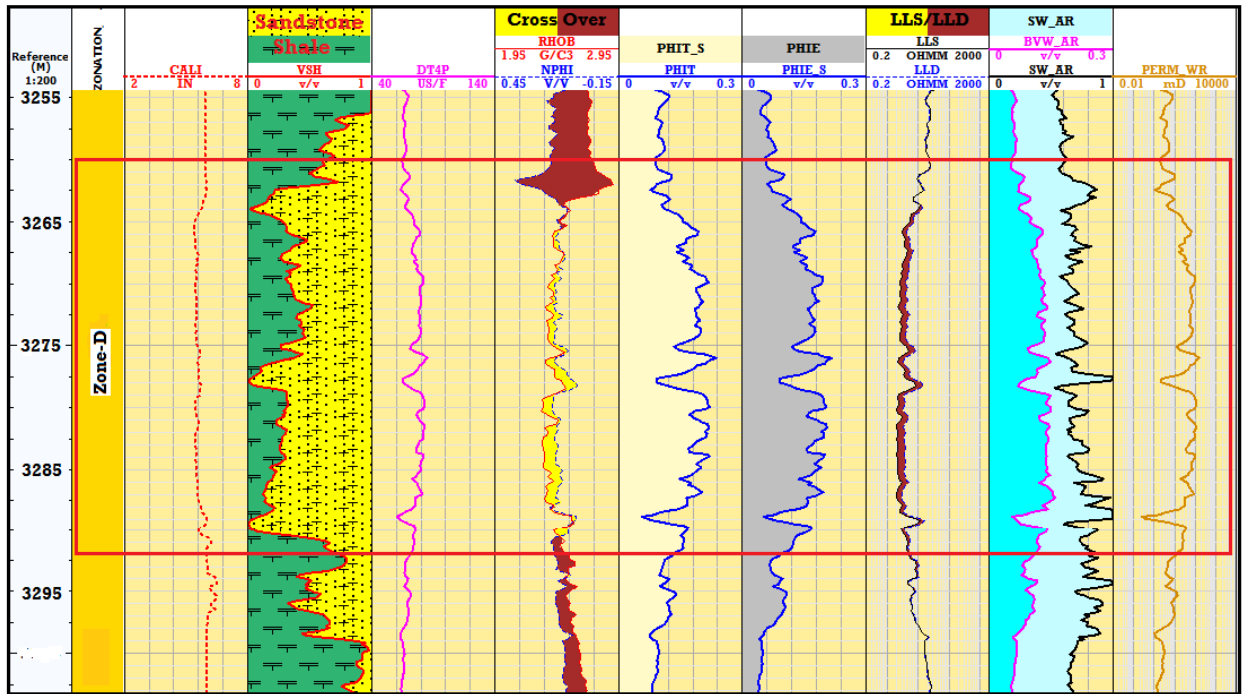
Figure 12: Composite log responses for well Sawan 05. The cross-over clearly indicates the reservoir zone, 3260-3290 m deep, within the C-sand interval.
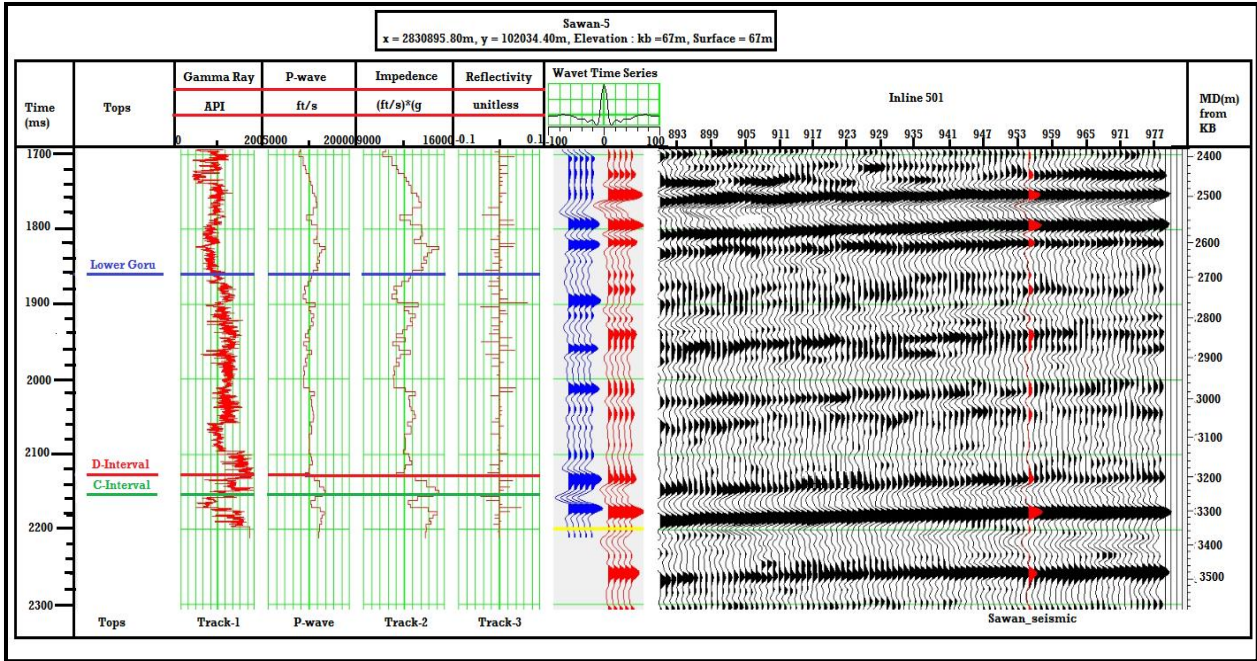
Figure 13: Generation of synthetic seismogram using data of well Sawan-05. Synthetic and extracted seismic traces, at the well location, are respectively shown in blue and red colours.
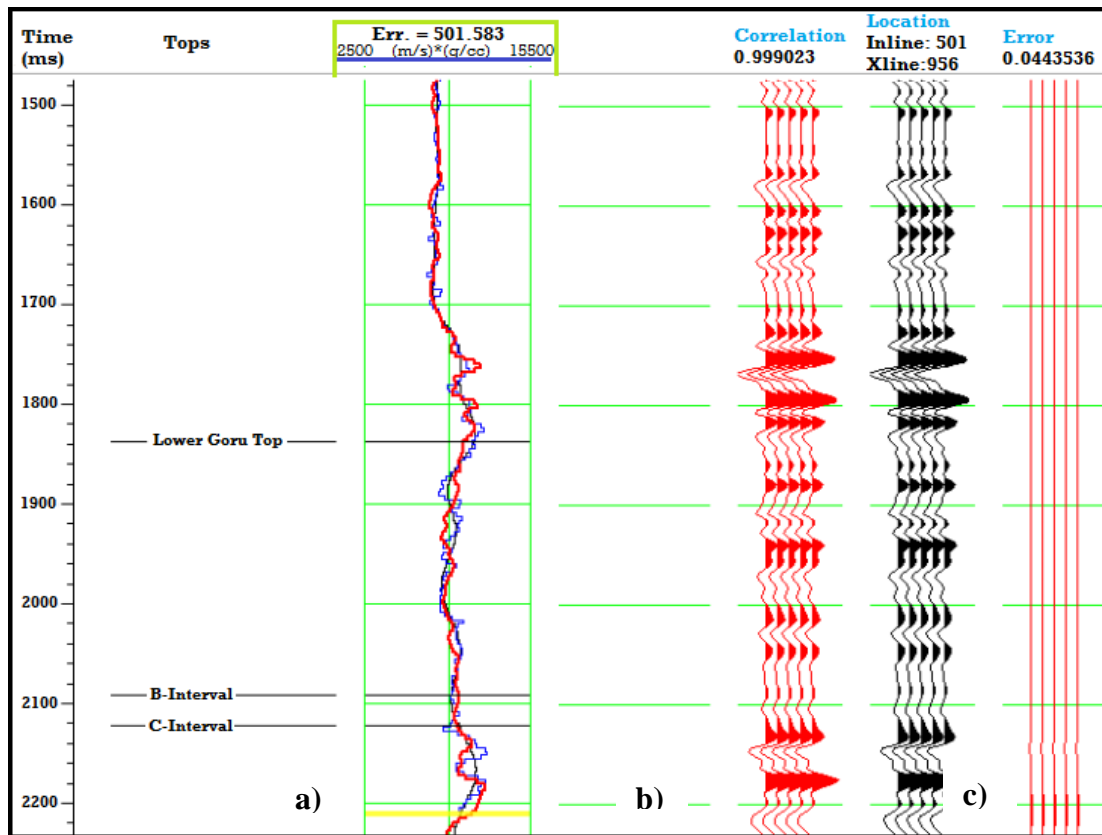
Figure 14: Analysis of the model-based post-stack seismic inversion at well Sawan-05 compared with the initial model: a) filtered impedance log (blue), initial model (black), inversion impedance log (red); b) synthetic trace from inversion (red) and extracted trace from the seismic (black). c) RMS error between the synthetic and seismic traces.
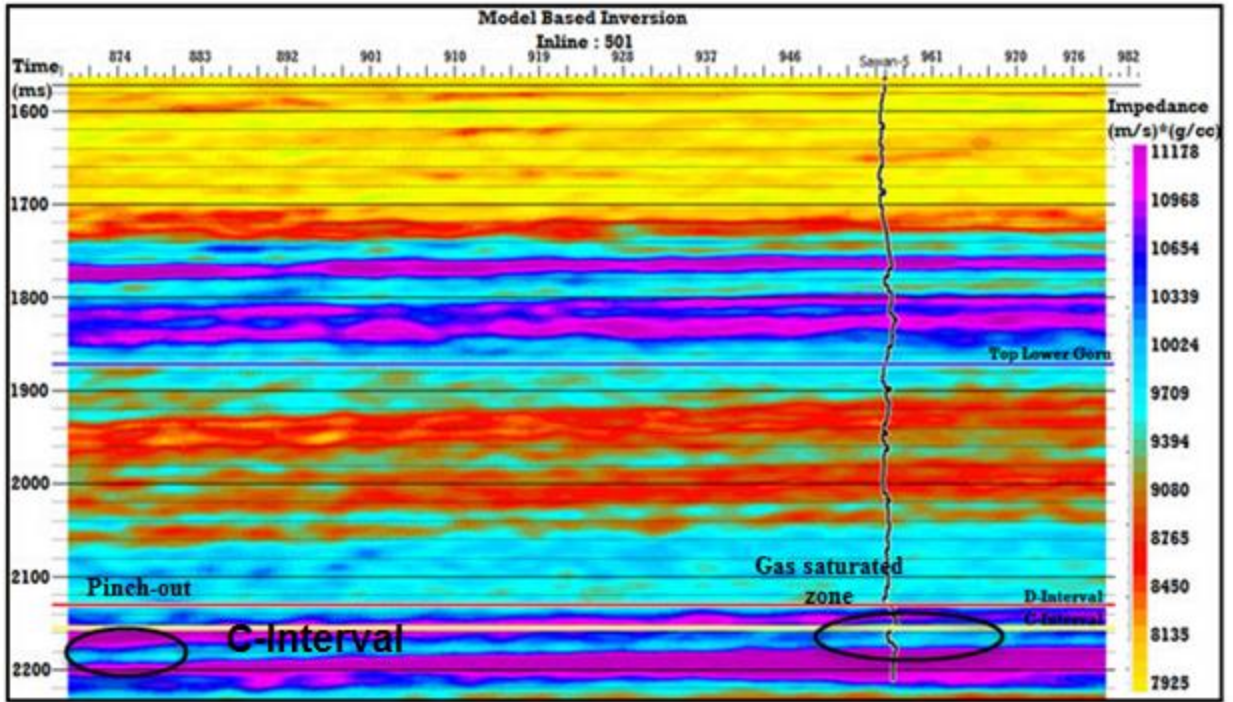
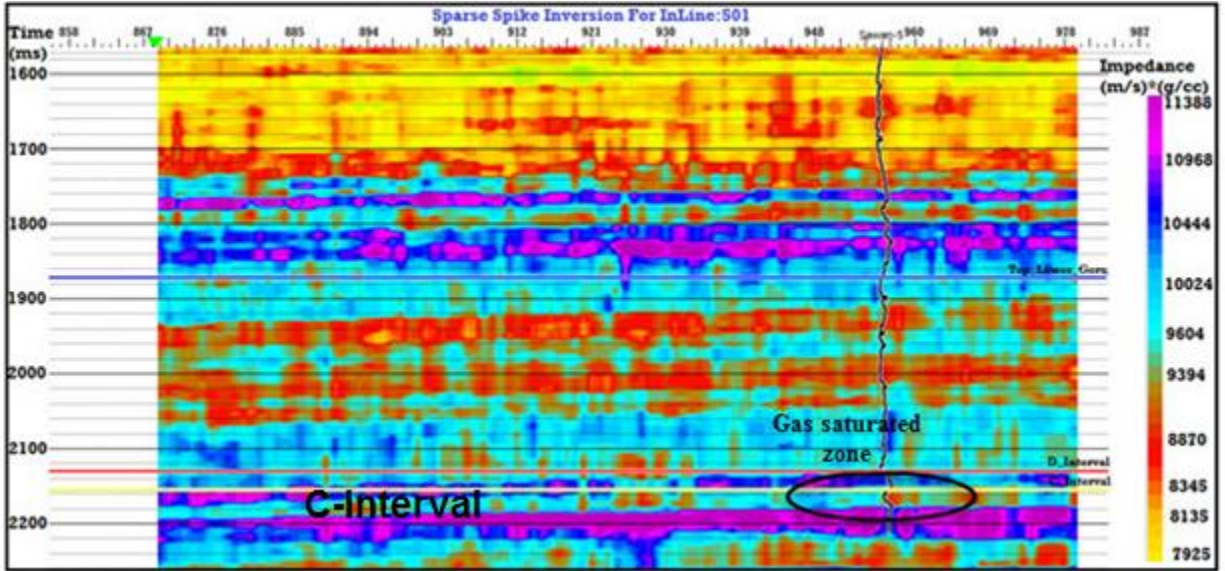Figure 15: Model-based inverted acoustic impedance for inline 501. The impedance log of well Sawan-05 is also shown at CDP 956. This inversion algorithm is able to capture detailed lateral variations in lithology.
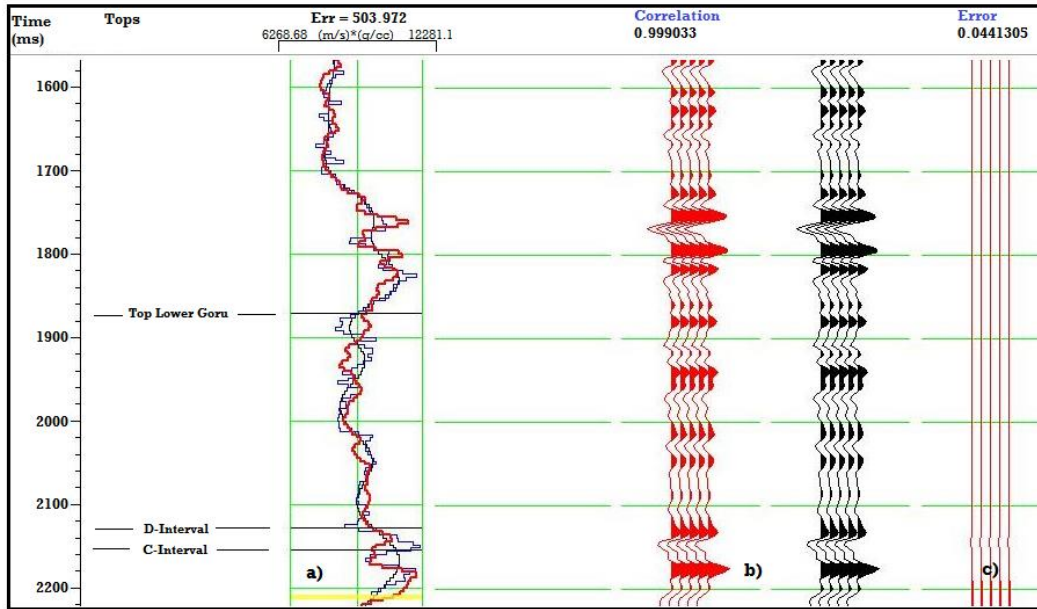
Figure 16: Analysis of sparse-spike post-stack inversion at well Sawan-05: a) filtered impedance log (blue), initial model (black), inverted acoustic impedance (red); b) synthetic trace from inversion (red) and extracted trace from the seismic (black). c) RMS error between the synthetic trae and seismic traces.

Figure 17: Sparse-spike based inverted acoustic impedance for inline 501. The impedance log of well Sawan-05 is also shown at CDP 956.
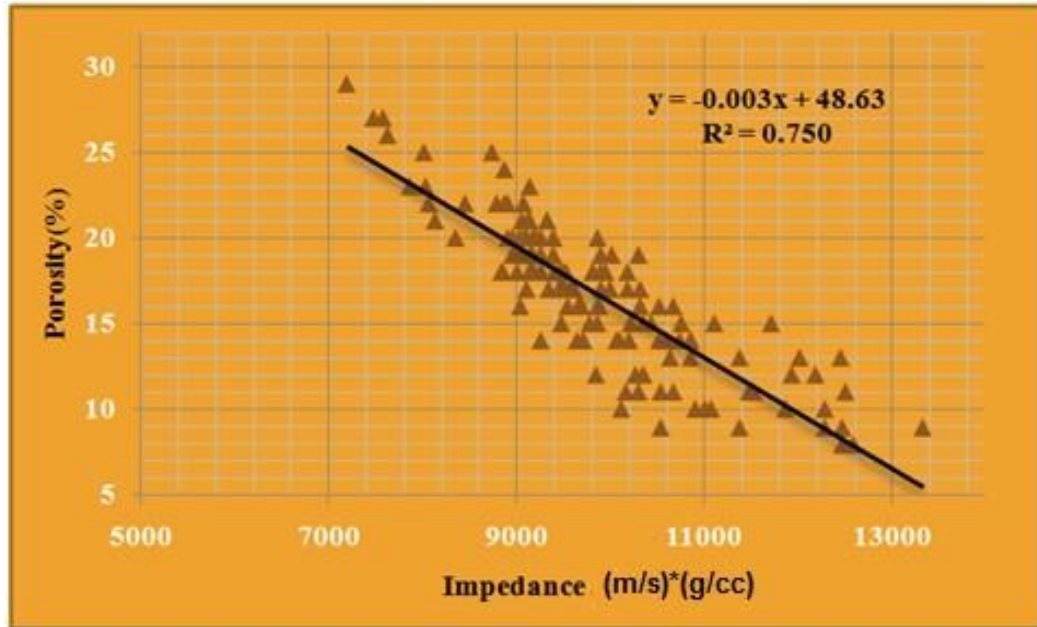
Figure 18: Cross plot of acoustic impedance (AI) and effective porosity with acceptable value of correlation coefficient. Porosity and acoustic impedance are always linearly related, showing a negative slope.
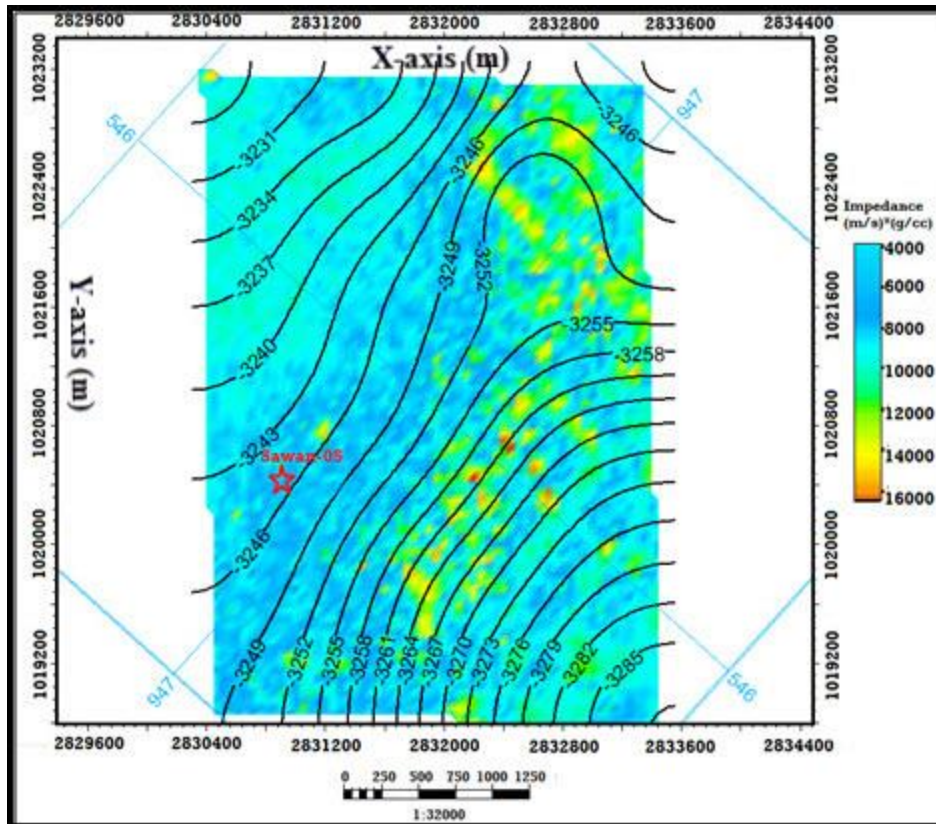
Figure 19: The acoustic impedance map of C-sand interval overlain by the depth contour map.
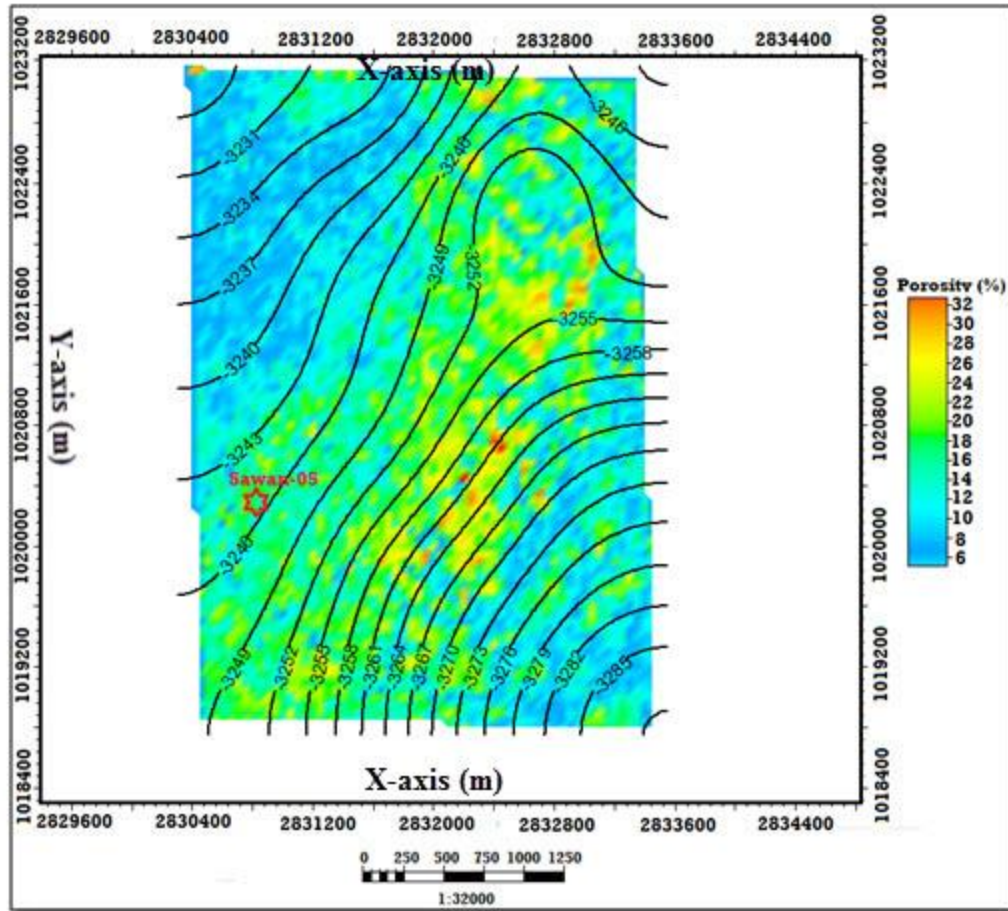
Figure 20: Porosity distribution in the C-sand interval as estimated from inverted impedance overlain by the depth contour map. At the location of well Sawan-05, the porosity extracted from the model-based inversion and petrophysical analyses are in good match.